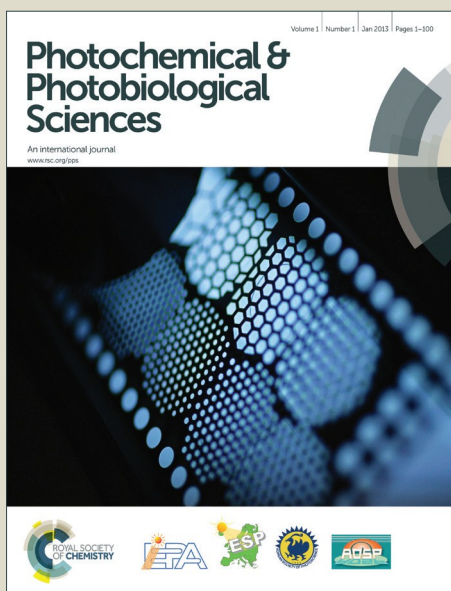


Photochemical & Photobiological Sciences

Accepted Manuscript



This is an *Accepted Manuscript*, which has been through the Royal Society of Chemistry peer review process and has been accepted for publication.

Accepted Manuscripts are published online shortly after acceptance, before technical editing, formatting and proof reading. Using this free service, authors can make their results available to the community, in citable form, before we publish the edited article. We will replace this *Accepted Manuscript* with the edited and formatted *Advance Article* as soon as it is available.

You can find more information about *Accepted Manuscripts* in the [Information for Authors](#).

Please note that technical editing may introduce minor changes to the text and/or graphics, which may alter content. The journal's standard [Terms & Conditions](#) and the [Ethical guidelines](#) still apply. In no event shall the Royal Society of Chemistry be held responsible for any errors or omissions in this *Accepted Manuscript* or any consequences arising from the use of any information it contains.

Relay Proton Transfer Triggered Twisted Intramolecular Charge Transfer

Santosh Kumar Behera and G. Krishnamoorthy*
Department of Chemistry
Indian Institute of Technology Guwahati
Guwahati, Assam 781039
India

E-mail: gkrishna@iitg.ernet.in

Abstract

The mechanism for the dual emission of 2-(4'-*N*, *N*-dimethylaminophenyl)imidazo[4,5-*c*]pyridine (DMAPIP-*c*) in protic solvents was investigated by synthesizing and studying its analogues. Theoretical calculations were carried out to corroborate the experimental findings. The deprotonation studies suggest that the enhancement in TICT emission of anionic form of DMAPIP-*c* is limited to protic environment. The spectral characteristics of DMAPIP-*c* were also studied in methanol-acetonitrile binary solvent mixture. Unlike DMAPIP-*c*, the methyl derivatives do not emit dual fluorescence in protic solvents. The relative intensity of the TICT emission (with respect to that of normal emission) rises with methanol amount in the acetonitrile–methanol binary solvent mixture. The studies also show that a 1:3 hydrogen bonded complex is formed between DMAPIP-*c* and methanol and it is responsible for the TICT emission. Based on the results a relay proton transfer triggered TICT emission is proposed. TDDFT calculations were performed to predict the emission energies.

Keywords: Proton Transfer, TICT, Hydrogen bond, Relay transfer, DFT calculations

1. Introduction

Intramolecular charge transfer (ICT) is an important excited state process in chemistry and biology.¹⁻³ Though several mechanisms were proposed to demonstrate formation of the ICT state, the twisted ICT (TICT) model proposed by Grabowski *et al.* is widely accepted. According to TICT model, the twisting of donor to a perpendicular geometry is associated with intramolecular charge transfer process.^{4,5} In other words, that the donor is perpendicular to other part of the molecule in the ICT state. It is well documented that the TICT emission depends on the polarity as well as that of viscosity.⁴⁻¹² A close look reveals that other than polarity and viscosity, the hydrogen bonding also strongly influence the TICT process of numerous systems.¹³⁻²⁰ Solvents can form hydrogen bond with either the charge donor or the charge acceptor of the molecule. Cazeau-Dubroca *et al.* hypothesized that the twisted conformer was formed in the ground state due to hydrogen bonding of the donor with the solvent and the twisted species upon excitation emits TICT emission.¹⁵ However, their hypothesis was severely challenged by experimental findings.^{16,17} But recently Dreuw *et al.* predicted that such a hydrogen bonding provides a path for energy dissipation in gaseous phase which enables the formation of TICT state in the gaseous phase.¹⁸ On the other hand, it is unambiguously established that the hydrogen bonding of the acceptor with the solvent favours the TICT process.^{13,19,20} The hydrogen bonding of the acceptor enhances the charge transfer from the donor to the acceptor thereby it promotes the ICT. Therefore, though it is not prerequisite the hydrogen bonding of the solvent with the acceptor boosts the TICT process in several dyes. The relationship between charge transfer and hydrogen bond formation is also a topic of current interest in several chemical and biological processes where hydrogen bond provokes proton coupled charge separation.²¹⁻²⁴

The TICT emission of 2-(4'-*N,N*-dimethylaminophenyl)imidazo[4,5-*c*]pyridine (DMAPIP-*c*, chart 1) is an attractive one.²⁵ Unlike other common TICT emitting molecules,

the protic environment is critical for DMAPIP-c to exhibit TICT emission. Even in polar aprotic solvents no TICT emission was observed from DMAPIP-c. Fasani *et al.* investigated the photophysical properties of the amino analogue of DMAPIP-c.²⁶ They observed that the molecule emits from the locally excited state as well as from the TICT state only in alcohols. But not in nonpolar or polar aprotic solvents. They conjectured that the protic solvent forms hydrogen bond with hydrogen of theazole 'NH' hydrogen and the nitrogen of imidazole, which twist the pyridoimidazole moiety (acceptor) perpendicular to form the TICT state. This acceptor twisting model was not supported by studies of Krishnamoorthy and Dogra.²⁵ Moreover the Fasani model did not assign any role for the pyridyl nitrogen in the TICT process. But, our earlier studies clearly established that the TICT emission be determined not only by the presence of pyridyl nitrogen but also by its' position.^{25,27} The AM1 calculation on DMAPIP-c predicted that under isolated condition, the imidazopyridine ring (the acceptor) is out of plane from the phenyl ring.²⁵ Further the calculations also predicted that the hydrogen bonding of the imidazopyridine ring (acceptor) with solvent make the imidazopyridine ring coplanar with phenyl ring. This led to the proposition that the planarization through hydrogen bonding increase the charge flow to acceptor from the phenyl ring that results in TICT state. But *ab initio* calculations on DMAPIP-c suggested that the phenyl and the imidazopyridine rings are planar even under isolated conditions.²⁷ This ruled out the planarization role for the protic solvents in formation of TICT state in 2-(4'-aminophenyl)imidazopyridines. Therefore, we have explored the characteristics of DMAPIP-c and related molecules (Chart 1) to comprehend the mechanism for the dual emission of DMAPIP-c in protic environment.

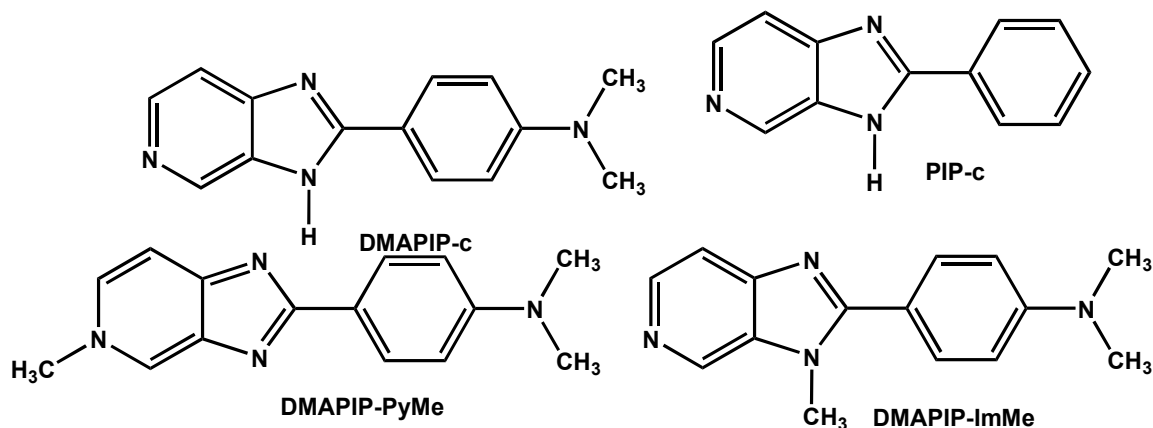


Chart 1. Structure of DMAPIP-c and its methyl derivatives, *N,N*-dimethyl-4-(1-methyl-1H-imidazo[4,5-c]pyridin-2-yl)benzenamine (DMAPIP-ImMe), *N,N*-dimethyl-4-(5-methyl-5H-imidazo[4,5-c]pyridin-2-yl)benzenamine (DMAPIP-PyMe) and 2-(phenyl)imidazo[4,5-c]pyridine (PIP-c).

2. Materials and Methods

2.1. 2-(4'-*N,N*-dimethylaminophenyl)imidazo[4,5-c]pyridine (DMAPIP-c)

DMAPIP-c was synthesized by following the procedure reported for similar compound.²⁸ A equimolar mixture of 3,4-diaminopyridine and 4-(*N,N*-dimethylamino)benzoic acid was refluxed in POCl₃ for 6 h. The cooled reaction mixture was added to ice cold water and neutralized with sodium hydroxide. The precipitate thus obtained was purified by column chromatography. The mass and NMR data confirmed the product.

¹H NMR (400 MHz, CDCl₃, ppm) δ 3.11 (6H, s), 6.89 (2H, d), 7.93 (1H, d), 8.20 (2H, d), d 8.34 (1H, d), 8.97 (1H, s)

HRMS (ESI) *m/z*: [M+ H]⁺ Calcd for C₁₄H₁₄N₄ 239.1252; Found 239.1301.

2.2. *N,N*-dimethyl-4-(5-methyl-5H-imidazo[4,5-c]pyridin-2-yl)benzenamine (DMAPIP-PyMe)

DMAPIP-c and methyl iodide were mixed completely and irradiated intermittently in a microwave oven at 200W for 4h.²⁹ After irradiation, the mixture was cooled and then treated

with base.³⁰ The product obtained was purified by preparative thin layer chromatography. The NMR and mass data confirmed the identity of the product.

¹H NMR (400 MHz, CDCl₃, ppm) δ 3.10 (3H, s), 3.53(6H, s), 4.02 (1H, d), 7.05 (2H, d), 7.08(2H, d), 7.48 (2H, m)

HRMS (ESI) m/z: [M+ H]⁺ Calcd for C₁₅H₁₆N₄ 253.1409; Found 253.1461.

2.3. *N,N*-dimethyl-4-(1-methyl-1H-imidazo[4,5-c]pyridin-2-yl)benzenamine (DMAPIP-ImMe)

DMAPIP-c, methyl iodide and KOH (powder) were dissolved in a 3:1 solvent mixture of dimethyl formamide and tetrahydrofuran. The mixture was heated at 40 °C with stirring for 20 h.³¹ The product obtained was purified by column chromatography and its identity was confirmed by mass and NMR data.

¹H NMR (400 MHz, CDCl₃, ppm) δ 3.07 (6H, s), 4.11 (3H, s), 6.65 (2H, d), 7.69 (2H, d), 7.77 (1H, d), 8.30 (2H, d)

HRMS (ESI) m/z: [M+ H]⁺ Calcd for C₁₅H₁₆N₄ 253.1409; Found 253.1448.

2.4. 2-(Phenyl)imidazo[4,5-c]pyridine (PIP-c)

PIP-c was prepared by refluxing benzoic acid and 3,4-diaminopyridine in polyphosphoric acid at 190°C for 5 h. The cooled reaction mixture was poured to ice cold water. The mixture was neutralized by potassium hydroxide solution. The dried solid product was recrystallized twice in methanol. The product was confirmed by HRMS mass and NMR data.

¹H NMR (600 MHz, CDCl₃, ppm) δ 8.86 (1H, s), 7.36 (4H, m), 8.08 (2H, dd), 8.22 (1H, d)

HRMS (ESI) m/z: [M+ H]⁺ Calcd for C₁₂H₉N₃ 196.0830; Found 196.0872.

2.5. Spectral measurements

Absorption spectra were recorded on a Varian Cary 100 UV-visible spectrometer and the steady state fluorescence spectra were measured on a Horiba Jobin Yvon Spex Fluoromax 4 spectrofluorimeter. HPLC grade solvents procured from Merck or Rankem (India) were used for the studies. The tetrabutyl ammonium fluoride and tetrabutyl ammonium chloride salts were procured from Sigma Aldrich, USA. Fluorescence lifetimes were measured on a time correlated single-photon counting (TCSPC) method based Life-Spec II instrument (Edinburgh Instrument) using 375 nm laser diode. The fluorescence decay was analysed by reconvolution method using the FAST software provided by Edinburgh instruments. The goodness of the exponential fits was evaluated on the basis of the reduced χ^2 value and residual plot. The fluorophore concentrations were either 1×10^{-5} M or saturated solution for the spectral measurements.

The Lippert–Mataga equation used for the analysis of solvent-dependent spectral shifts is given below,³²

$$\bar{\nu}_{ss} = \left[\frac{2(\mu_e - \mu_g)^2}{hca^3} \right] \Delta f + \text{Constant} \quad (1)$$

Where $\bar{\nu}_{ss} = \bar{\nu}_{\max}^{ab} - \bar{\nu}_{\max}^{fl}$, is the Stokes shift, h is the Planck's constant, c is the speed of light, μ_e and μ_g are the excited state and ground state dipole moments of the dye, respectively and a denotes the Onsagar cavity radius. The orientation polarizability is defined by

$$\Delta f = \left[\frac{\varepsilon - 1}{2\varepsilon + 1} - \frac{n^2 - 1}{2n + 1} \right] \quad (2)$$

where ε and n are the dielectric constant and refractive index of the solvent, respectively.

2.6. Computational Details

The calculations were performed by using Gaussian 09 program.³³ Integral equation formalism-polarizable continuum (IEF-PCM) model is used to include the solvent stabilization by choosing methanol as solvent.^{34,35} The configuration interaction with single excitations (CIS) method is used for optimization of excited state geometry of the molecules.³⁶ In recent times for the electronic structure calculations in the excited states time-dependent density functional theory (TDDFT) is most popular method. The combination of efficiency, that is, computational cost, as well as precision makes TDDFT very popular.^{37,38} The TDDFT calculations were performed on the optimized structure to obtain molecular energy. The approach was successful to predict molecular parameters in number of systems.^{39,40} In addition the structures are fully optimized in the first excited state by TDDFT method using different functions such as Becke's three-parameter hybrid functional B3LYP, Coulomb-attenuating method (CAM)-B3LYP and B3LYP-D3 to obtain the molecular energy.⁴¹⁻⁴⁴ The 6-31G (d, p) basis set were employed for the calculations. The energies thus obtained for normal emission are compiled in Table 1.

3. RESULT AND DISCUSSION

3.1. Spectral characteristics of methyl derivatives

The methyl derivatives of DMAPIP-c were synthesized to ascertain the role of hydrogen bonding of the solvent with imidazole 'NH' hydrogen and pyridyl nitrogen in the longer wavelength emission processes. The emission and the excitation spectra of methyl derivatives in cyclohexane have well resolved vibronic structures with vibrational frequency $2500 \pm 100 \text{ cm}^{-1}$ and $1650 \pm 100 \text{ cm}^{-1}$ (ESI, Fig. S1 and S2). The good mirror image relationship between the excitation and emission spectra suggests that both the band corresponds to the same electronic transition i.e. S_0-S_1 . When polarity and hydrogen bonding capacity of the solvent is increased the spectra are blurred and bathochromic shifts are

observed (Table 2, Fig. 1 and 2, ESI, Fig. S3 and S4). These features of the methyl derivatives are same as those of DMAPIP-c. However the solvatochromic shifts in the spectra of the methyl derivatives are less as compared to those of DMAPIP-c.

The μ_e of the methyl derivatives are calculated using Lippert-Mataga plots (Fig S5). The excited state dipole moments of DMAPIP-ImMe, and DMAPIP-PyMe thus obtained are 9.9 and 7.7 D, respectively. Smaller μ_e of methylated derivatives compared to that of DMAPIP-c (12.0 D)²⁵ indicates that charge transfer process is affected by the methylation of pyridyl nitrogen as well as that of imidazole 'NH' group.

Interestingly, no dual emission is observed in both methyl derivatives. However, some time a weak emission may be buried underneath the strong normal emission. Even in DMAPIP-c, though clear dual emission is not observed in solvent such as propanol the time resolved studies indicated the weak TICT emission is submerged under the normal emission. Therefore, the fluorescence decays of the methyl derivatives were measured (Table 2). In aprotic solvents, the fluorescence decay of DMAPIP-c was monoexponential, nevertheless it was double exponential in protic solvents.²⁵ But the fluorescence decays of methyl derivatives are monoexponential in aprotic as well as protic solvents. This shows that dual emission is not observed in the methyl derivatives. Due to methylation the hydrogen bonding with pyridyl nitrogen and imidazole 'NH' hydrogen are not feasible in DMAPIP-PyMe and DMAPIP-ImMe, respectively. Therefore, the no longer wavelength emission in methyl derivatives specifies that the hydrogen bonding of both azole 'NH' hydrogen and pyridyl nitrogen with the solvent are essential for the dual emission of DMAPIP-c. The proton transfer from the azole 'NH' hydrogen to the pyridyl nitrogen is one such process which requires the hydrogen bonding of solvents at both azole 'NH' hydrogen and pyridyl nitrogen. In the excited state, the transfer of proton from the acidic group to the basic group occurs through hydrogen bonding and it often results in dual emission.⁴⁵⁻⁴⁹ Usually a negative

solvatochromism is observed in the tautomer fluorescence that formed by proton transfer. However, the longer wavelength fluorescence of DMAPIP-c is a TICT emission and it exhibits strong positive solvatochromism. A red shift was observed in the longer wavelength emission in water compare to that of methanol and strong blue shift was observed in the longer wavelength emission on moving from the more polar to less polar environment.^{25,50,51} Nonetheless in some cases positive solvatochromism is observed when the proton transfer assist the ICT process.⁵²⁻⁵⁴

3.2. The relay proton transfer

In 7-hydroxyquinoline-8-carbaldehydes the relay proton transfer was reported to take place via ionic form.⁵⁵ In DMAPIP-c also the proton transfer might involve deprotonation at imidazole 'NH' proton followed by its addition at pyridyl nitrogen. The effect of deprotonation on the spectral characteristics of DMAPIP-c in aqueous solution was already investigated.⁵⁶ Though the absorption spectrum and the normal emission of the anion are blue shifted compared to neutral molecule no shift was observed in its' longer wavelength emission. But, the intensity of the longer wavelength fluorescence of DMAPIP-c enhanced upon deprotonation. These results suggest that the species responsible for the longer wavelength emission in both anion and neutral species is same. Therefore, it may be hypothesized that the molecule that was deprotonated in the ground state to form anion and was again protonated in the excited state. If reprotonation occurs at same site, one should expect no shift in the normal emission also. The blue shift in the normal emission of the anion with respect to neutral form indicates that reprotonation did not occur at same site. Further, the enhancement in the longer wavelength emission suggests that the deprotonation is one of the steps that lead to the longer wavelength emitting state. In DMAPIP-c single solvent molecule is not sufficient to produce the biproton transfer and this should occur via solvent network. To verify the relay proton transfer hypothesize we deprotonated DMAPIP-c with fluoride

anion in acetonitrile. Since acetonitrile is an aprotic solvent whose polarity similar to that of methanol it is expected to prevent the relay proton transfer without hindering the charge transfer process. Upon addition of fluoride the absorption and the fluorescence spectra are blue shifted due to formation of anion (Fig. 3 and 4). However, no longer wavelength fluorescence is observed in presence of fluoride (Fig. 4). Similar study with chloride ion (relatively weaker base) does not produce any shift in the absorption and fluorescence spectra of DMAPIP-c (Fig. S6). This confirms the fact that the spectral shift observed upon addition of fluoride ion is not due to the effect of ionic strength but due to formation of anion.

The results are summarized below: (i) the non-appearance of longer wavelength emission in methyl derivatives shows that hydrogen bonding of the solvents with both azole 'NH' hydrogen and pyridyl nitrogen and play essential roles in formation of TICT state (ii) the enhancement in TICT emission upon deprotonation in aqueous medium and its absence upon deprotonation in polar aprotic solvent signifies the role of relay proton transfer in the process. (iii) Strong positive solvatochromism advocates that the relay proton transfer leads to a TICT state. Based on these, a scheme for the formation of TICT state is proposed (Scheme 1). The scheme was substantiated by the fact that the TICT emission for both neutral and anion are same. This relay proton transfer is a paramount interesting process and it can mimicking proton relay in vital biosystems.⁵⁷

3.3. Binary solvent mixture and stoichiometry

The spectral characteristics of DMAPIP-c in neat solvents were reported else where.²⁵ A bathochromic shift was observed in the absorption spectra upon increase in polarity and hydrogen bonding capacity of the solvents except in water. Here, the effect of acetonitrile-methanol binary solvent mixture on the absorption spectrum of DMAPIP-c is investigated (Fig. 5). Successive addition of methanol to acetonitrile shift the absorption spectrum of

DMAPIP-c towards longer wavelength. This red shift is the consequence of hydrogen bonded complex formation of methanol with DMAPIP-c.

The relay proton transfer process involves cyclic hydrogen bonding network of fluorophore and solvent molecules. For eg., relay proton transfer of 7-hydroxyquinoline and 3-hydroxyxanthone involves cyclic network of two and three solvent molecules, respectively.^{58,59} Therefore, to determine the number of methanol molecules those act as bridge connecting the 'NH' group and pyridyl nitrogen in the relay transfer, the fluorescence characteristics are investigated in acetonitrile-methanol mixture. DMAPIP-c emits a single emission at 390 nm in acetonitrile and is consistent with the earlier work.²⁵ Gradual addition of methanol lead to formation of an additional band at longer wavelength. The relative intensity of the longer wavelength band increases with increases in quantity of methanol (Fig. 6). Though at low methanol concentration, the longer emission band is not clear, the band is well developed with sequential addition of methanol. The emission spectrum of DMAPIP-c in neat methanol matches with the literature report.²⁵

The stoichiometric ratio of DMAPIP-c and methanol is estimated from the Benesi-Hildebrand plot (Fig. 7).⁶⁰ Since, we want to determine the stoichiometry of complex responsible for the TICT emission the fluorescence intensities at 550 nm is used for calculations. The general form of Benesi-Hildebrand equation for a 1: n complex formed between dye and methanol is presented below:

$$\frac{1}{I - I_0} = \frac{1}{I_\infty - I_0} + \frac{1}{K[M]^n \{I_\infty - I_0\}} \quad (3)$$

where [M] represents the concentration of methanol, I_0 and I are the fluorescence intensities in absence and presence of alcohol respectively, I_∞ is the limiting intensity of fluorescence, n is the number of methanol molecules and K is the binding constant. The plots of

$\frac{1}{I-I_0}V_S\frac{1}{[M]}$ and $\frac{1}{I-I_0}V_S\frac{1}{[M]^2}$ did not yield straight lines. However, the plot of

$\frac{1}{I-I_0}V_S\frac{1}{[M]^3}$ results in a straight line ($r^2 = 0.995$, Fig. 7). This advocates that three

methanol molecules are involved in the proton transfer process. The multiple proton-transfer systems are rare compared to single or two proton transfer and typically entail molecular self-assembly or assembly of solvent molecules.

Strong positive solvatochromism clearly suggests that the longer wavelength emission is TICT emission. Still to rule out that the emission is not due to relay proton transfer without charge transfer we synthesized, 2-phenylimidazo[4,5-c]pyridine (PIP-c) without the charge donating dimethylamino group. The spectral characteristics of PIP-c were studied in acetonitrile-methanol mixture. The longer wavelength emission is observed neither in acetonitrile-methanol mixture nor in pure solvents (Fig. 8). Unlike in DMAPIP-c with addition of methanol only a blue shift is observed even in normal emission of PIP-c. Thus, our conclusion that the longer wavelength is due to emission of the TICT state is further substantiated.

3.4. Quantum mechanical calculations

As mentioned earlier, the structure of the complex were optimized in the excited state by CIS and TDDFT methods and the emission energy of the normal emission is calculated by TDDFT method using different functions. The normal emission predicted from the TDDFT (with B3LYP-D3 function) optimized structure is better agreement with the experimental value. Therefore, this procedure was followed for the excited state optimization of different forms of DMAPIP-c.(CH₃OH)₃ complex (Fig. 9). The calculations also suggest that three methanol molecules are required to form the cyclic hydrogen bond structure. In the normal form complex the H₁₇⋯O₁₈ and H₂₃⋯N₆ hydrogen bond lengths are 1.93 Å and 1.77 Å, respectively. In H₁₇⋯O₁₈ hydrogen bond the hydrogen atom of the imidazole 'NH' group

acts as the hydrogen bond donor and the oxygen atom of the methanol acts as the hydrogen bond acceptor. In $H_{23}\cdots N_6$ hydrogen bond, the hydrogen atom of the methanol acts as the hydrogen bond donor and the pyridyl nitrogen acts as the hydrogen bond acceptor. The $H_{17}-O_{18}$ and $H_{23}-N_6$ bond distances shrink to form covalent bonds and the $N_1\cdots H_{17}$ and $O_{22}\cdots H_{23}$ bond distances elongate as hydrogen bond to form tautomer. In tautomer- $(CH_3OH)_3$ complex $N_1\cdots H_{17}$ and $O_{22}\cdots H_{23}$ hydrogen bonds are 1.70 Å and 2.22 Å respectively. In all the complexes, the $N-H\cdots O$ hydrogen bonds are little longer than $O-H\cdots N$ hydrogen bonds. In other words, methanol formed a shorter bond when it acts as hydrogen bond donor than when it acts as hydrogen bond acceptor. The intermolecular hydrogen bond between two methanol molecules ($O-H\cdots H$ hydrogen bond) are shorter than 2 Å. The intermolecular hydrogen bond between methanol molecules also affected by the formation of tautomer. The cone angles of tautomer- $(CH_3OH)_3$ complex are $\angle N_1\cdots H_{17}-O_{18} = 166^\circ$, $\angle O_{18}\cdots H_{19}-O_{20} = 176^\circ$, $\angle O_{20}\cdots H_{21}-O_{22} = 174^\circ$, $\angle O_{22}\cdots H_{23}-N_6 = 131^\circ$ and those of normal- $(CH_3OH)_3$ complex are $\angle N_1-H_{17}\cdots O_{18} = 148^\circ$, $\angle O_{18}-H_{19}\cdots O_{20} = 177^\circ$, $\angle O_{20}-H_{21}\cdots O_{22} = 173^\circ$, $\angle O_{22}-H_{23}\cdots N_6 = 158^\circ$. Twisting of dimethylamino group shortens these hydrogen bonds. In other words, the formation of TICT strengthened the hydrogen bonds of the imidazo pyridine ring (acceptor). But still the hydrogen bond is little shorter when methanol acts as donor than when it acts as acceptor. The bond distances and cone angles are suitable for the hydrogen bond formation in both complexes.⁶¹

The emission energy obtained from the theoretical calculations are sketched in Scheme 2. The calculations predict that the energy of normal hydrogen bonded structure is lowest in the ground state. But in the excited state, the energy of the normal form is higher than that of the tautomer. This suggests that the relay proton transfer through solvent molecule is energetically favoured in the excited state. From the tautomer, twisting of the dimethylamino group or the dimethylaminophenyl group should lead to TICT state.

Therefore, the energies of both the excited states were calculated. In the S_1 state, the energy of the dimethylamino twisted conformer is less than that of the dimethylaminophenyl twisted conformer. Thus, it can be inferred that it is the dimethylamino group that is twisted to form the TICT state in DMAPIP-c. The energy predicted by the calculation for the TICT emission (2.41 eV) is also concord with the experimental value (2.61 eV) in methanol.²⁵ The frontier molecular orbitals involved in this transition are shown in Figure 10. The charge localized on the dimethylamino group in the highest occupied molecular orbital (HOMO) and on the other part of the molecule in the lowest unoccupied molecular orbital (LUMO). This decoupled orbitals (very little overlap between these orbital) are consistent with TICT model.⁴

The proton transfer induced charge transfer that lead to nonradiative process was reported in number of molecules.^{13,62} Similar proton transfer enhanced/induced TICT emission was reported from 4-amino- and 4-*N,N*-dimethylamino- salicylic acids.^{40,63} But in salicylic acids the proton transfer is an intramolecular process, the salient feature in DMAPIP-c is that it is an intermolecular process involves relay of four proton transfer which leads to TICT emission.

4. CONCLUSION

No dual emission is observed when pyridyl nitrogen or imidazole 'NH' of DMAPIP-c can not form hydrogen bond. The binary solvent study reveals that three solvent molecules are involved in the formation of TICT state. No TICT emission is observed upon deprotonation in acetonitrile. Comparison of characteristics of anionic form in protic and aprotic solvents indicates that the formation of TICT state occurs via monoanionic form, but the anion does not emit TICT emission in aprotic solvent. The relay transfer of proton from the imidazole hydrogen to the nitrogen at pyridyl ring induces the TICT emission in DMAPIP-c. In contrary to Fasani *et al.* model, the dimethylamino group of DMAPIP-c is twisted to form the

TICT state. The theoretical calculations support the proposed mechanism and the transition energy predicted by the calculation is in good agreement with experimental value.

Acknowledgement

The authors thank Department of Science and Technology (DST), New Delhi for the financial support of the project SR/S1/PC/0046/2010. The authors also acknowledge the Central Instruments Facility (CIF), Indian Institute of Technology Guwahati for the NMR, LCMS and fluorescence lifetime measurements.

Electronic supplementary information (ESI) available: The plots showing mirror image relationship between the excitation and emission spectra for DMAPIP-PyMe and DMAPIP-ImMe in cyclohexane. The normalized excitation spectra of DMAPIP-PyMe and DMAPIP-ImMe in different solvents and the Lippert-Mataga Plot for DMAPIP-PyMe and DMAPIP-ImMe. The absorption and fluorescence spectra of DMAPIP-c in presence of chloride ion.

References

1. W. Rettig, *Electron Transfer I*, Topics in current chemistry; Springer-Verlag: Berlin, 1994, vol. 169, pp 253–299.
2. G. Campi, G. Ciasca, N. Poccia, A. Ricci, M. Fratini, and A. Bianconi, Controlling photoinduced electron transfer via effects self-organization for novel functional macromolecular systems, *Curr. Protein. Pept Sci.*, 2014, **15**, 394-399.
3. T. Debnath, P. Maity, H. Lobo, B. Singh, G. S. Shankarling, and H. N. Ghosh, Extensive reduction in back electron transfer in twisted intramolecular charge-transfer (TICT) coumarin-dye-sensitized TiO₂ nanoparticles/film: A femtosecond transient absorption study. *Chem. A. Eur. J.*, 2014, **20**, 3510-3519.

4. Z. R. Grabowski, K. Rotkiewicz, and W. Rettig, Structural changes accompanying intramolecular electron transfer: Focus on twisted intramolecular charge transfer states and structures, *Chem. Rev.*, 2003, **103**, 3899–4031.
5. W. Rettig, Charge separation in excited states of decoupled systems-TICT compounds and implications regarding the development of new laser dyes and the primary process of vision and photosynthesis, *Angew. Chem., Int. Ed. Engl.*, 1986, **25**, 971–988.
6. D. J. Stewart, M. J. Dalton, R. N. Swiger, J. L. Fore, M. A. Walker, T. M. Cooper, J. E. Haley, and L.-S. Tan, Symmetry- and solvent-dependent photophysics of fluorenes containing donor and acceptor groups, *J. Phys. Chem. A.*, 2014, **118**, 5228-5237.
7. J. Catalan, On the dual emission of p-dimethylaminobenzonitrile and its photophysical implications, *Phys. Chem. Chem. Phys.*, 2013, **15**, 8811-8820.
8. F. Zhou, J. Shao, Y. Yang, J. Zhao, H. Guo, X. Li, S. Ji, and Z. Zhang, Molecular rotors as fluorescent viscosity sensors: Molecular design, polarity sensitivity, dipole moments changes, screening solvents, and deactivation channel of the excited states, *Eur., J. Org. Chem.*, 2011, **25**, 4773-4787.
9. N. Hobeika, J. – P. Malval, H. Chaumeil, V. Roucoules, F. Morlet - Savary, D. Le Nouen, and F. Gritti, Abnormal enhancement of the photoisomerization process in a trans-nitroalkoxystilbene dimers in beta-cyclodextrin cavities, *J. Phys. Chem. A*, 2012, **116**, 10328-10337.
10. F. S. Santos, R. R. Descalzo, P. F. B. Goncalves, E.V. Benvenuti, and F. S. Rodembusch, Evidence for excited state intramolecular charge transfer in benzazole-based pseudo-stilbenes, *Phys. Chem. Chem. Phys.*, 2012, **14**, 10994-11001.

11. K. S. Ramini, B. Anderson, S. – T. Hung, and M. G. Kuzyk, Experimental tests of a new correlated chromophore domain model of self-healing in a dye-doped polymer, *Polym. Chem.*, 2013, **4**, 4948-4954.
12. H. Kumar, A. Chattopadhyay, R. Prasath, V. Devaraji, R. Joshi, P. Bhavana, P. Saini, and S. K. Ghosh, Physicochemical Studies, solvation, and DNA damage of quinoline-appended chalcone derivative: Comprehensive spectroscopic approach toward drug discovery, *J. Phys. Chem. B*, 2014, **118**, 7257-7266.
13. F. A. S Chipem, A. Mishra, and G. Krishnamoorthy, The role of hydrogen bonding in excited state intramolecular charge transfer, *Phys. Chem. Chem. Phys.* 2012, **14**, 8775 - 8790.
14. M. Cigan, J. Donovalova, V. Szoecs, J. Gaspar, K. Jakusova, and A. Gaplovsky, 7-(Dimethylamino) Coumarin-3-Carbaldehyde and its Phenylsemicarbazone: TICT excited state modulation, fluorescent H-aggregates, and preferential solvation, *J. Phys. Chem. A.*, 2013, **117**, 4870 - 4883.
15. C. Cazeau-Dubroca, S. Ait Lyazidi, P. Cambou, A. Peirigua, Ph. Cazeau, and M. Pesquer, Twisted internal charge-transfer molecules- already twisted in the ground State., *J. Phys. Chem.*, 1989, **93**, 2347-2358.
16. K. A. Al-Hassan, and T. Azumi, The role of free-volume in the twisted intramolecular charge-transfer (TICT) emission of dimethylaminobenzonitrile and related-compounds in rigid polymer matrices., *Chem. Phys. Lett.*, 1988, **146**, 121-124.
17. T. Kobayashi, and M. Futakami, and O. Kajimoto, 4-(N,N-Dimethylamino)benzonitrile solvated by apolar molecule - structural demand for charge - transfer state formation, *Chem. Phys. Lett.*, 1986, **130**, 63 - 66.

18. M. Zakharov, O. Krauss, Y. Nosenko, B. B. Brutschy and A. Dreuw, Specific microsolvation triggers dissociation-mediated anomalous red-shifted fluorescence in the gas phase, *J. Am. Chem. Soc.*, 2009, **131**, 461–469.
19. A. Demeter, V. Mile, and T. Bérces, Hydrogen bond formation between 4-(Dimethylamino)pyridine and aliphatic alcohols, *J. Phys. Chem. A*, 2007, **111**, 8942 - 8949.
20. J. Herbich and J. Waluk, Excited charge transfer states in 4-Aminopyrimidines, 4-(dimethylanilino)pyrimidine and 4-(Dimethylamino)pyridine, *Chem. Phys.*, 1994, **188**, 247-265.
21. N. Cox, D. A. Pantazis, F. Neese, and W. Lubitz, Biological water oxidation, *Acc. Chem. Res.*, 2013, **46**, 1588-1596.
22. A. Migliore, N. F. Polizzi, M. J. Therie, and D. Beratan, Biochemistry and theory of proton-coupled electron transfer, *Chem. Rev.*, 2014, **114**, 3381-3465.
23. J. P. Layfield and S. Hammes-Schiffer, Hydrogen tunnelling in enzymes and biomimetic models, *Chem. Rev.*, 2014, **114**, 3466-3494.
24. A. P. Demchenko, K. -C. Tang and P. - T. Chou, Excited-state proton coupled charge transfer modulated by molecular structure and media polarization, *Chem. Soc. Rev.*, 2013, **42**, 1379-1408.
25. G. Krishnamoorthy and S. K. Dogra, Dual fluorescence of 2-(4'-N,N-Dimethylaminophenyl)pyrido[3,4-d]imidazole:effect of solvents, *Spectrochim. Acta A*, 1999, **55**, 2647-2658.
26. E. Fasani, A. Albini, P. Savarino, G. Viscardi, and E. Barni, Hydrogen bonding, protonation and twisting in the singlet excited state of some 2-(4-Aminophenyl)pyrido-oxa-, -thia-, and -imidazoles, *J. Heterocycl. Chem.*, 1993, **30**, 1041–1044.

27. N. Dash, F. A. S. Chipem, R. Swaminathan, and G. Krishnamoorthy, Hydrogen bond induced twisted intramolecular charge transfer in 2-(4-N,N-Dimethylaminophenyl)imidazo[4,5-b]pyridine, *Chem. Phys. Lett.*, 2008, **460**, 119-124.
28. V. Bavetsias, C. Sun, N. Bouloc, J. Reynisson, P. Workman, S. Linardopoulos, and M. Edward, Hit Generation and exploration: Imidazo[4,5-b]pyridine derivatives as inhibitors of aurora kinases, *Bioorg. Med. Chem. Lett.*, 2007, **17**, 6567–6571.
29. H. Yu, H. Kawanishi, and H. Koshima, Preparation and photophysical properties of benzimidazole-based gels, *J. Photochem. Photobiol. A: Chem.*, 2006, **178**, 62-69.
30. F. Wu, C. M. Chamchoumis, and R. P Thummel, Bidentate ligands that contain pyrrole in place of pyridine, *Inorg. Chem.*, 2000, **39**, 584-590.
31. Y. - P. Tong, S. - L. Zheng, and X. - M. Chen, Syntheses, structures, photoluminescence and theoretical studies of two dimeric Zn(II) Compounds with aromatic N,O-chelate phenolic ligands, *J. Mol. Struct.* 2007, **826**, 104-112.
32. E. Lippert, Spektroskopische bestimmung des dipolmomentes aromatischer verbindungen im ersten angeregten singulettzustand, *Z. Elektrochem.* 1957, **61**, 962–975.
33. Frisch, M. J.; Trucks, G. W.; Schlegel, H. B.; Scuseria, G. E.; Robb, M. A.; Cheeseman, J. R.; Scalmani, G.; Barone, V.; Mennucci, B.; Petersson, G. A. ; Nakatsuji, H.; Caricato, M.; Li, X.; Hratchian, H. P.; Izmaylov, A. F.; Bloino, J.; Zheng, G.; Sonnenberg, J. L.; Hada, M.; Ehara, M.; Toyota, K.; Fukuda, R.; Hasegawa, J.; Ishida, M.; Nakajima, T.; Honda; Kitao, Y. O.; Nakai, H.; Vreven, T.; Montgomery, J. A.; Jr.; Peralta, J. E.; Ogliaro, F.; Bearpark, M.; Heyd, J. J.; Brothers, E.; Kudin, K. N.; Staroverov, V. N.; Keith, T.; Kobayashi, R.; Normand, J.;

Raghavachari, K.; Rendell, A.; Burant, J. C.; Iyengar, S. S.; Tomasi, J.; Cossi, M.; Rega, N.; Millam, J. M.; Klene, M.; Knox, J. E.; Cross, J. B.; Bakken, V.; Adamo, C.; Jaramillo, J.; Gomperts, R.; Stratmann, R. E.; Yazyev, O.; Austin, A. J.; Cammi, R.; Pomelli, C.; Ochterski, J. W.; Martin, R. L.; Morokuma, K.; Zakrzewski, V. G.; Voth, G. A.; Salvador, P.; Dannenberg, J. J.; Dapprich, S.; Daniels, A. D.; Farkas, O.; Foresman, J. B.; Ortiz, J. V.; Cioslowski, J.; Fox, D. J. *Gaussian 09*, Revision D.01, Gaussian, Inc., Wallingford CT, **2013**.

34. S. Miertuš, E. Scrocco, and J. Tomasi, Static interaction of a solute with a continuum - A direct utilization of abinitio molecular potentials for the prevision of solvent effects, *Chem. Phys.*, 1981, **55**, 117-129.
35. E. Cancès, B. Mennucci, and J. Tomasi, A new integral equation formalism for the polarizable continuum model: Theoretical background and applications to isotropic and anisotropic dielectrics, *J. Chem. Phys.*, 1997, **107**, 3032-3041.
36. J. B. Foresman, M. Head-Gordon, J. A. Pople, and M. J. Frisch, Toward a Systematic Molecular Orbital Theory for Excited States, *J. Phys. Chem.*, 1992, **96**, 135-149.
37. M. E. Casida, *Time-dependent density-functional response theory for molecules, in Recent advances in density functional methods, Part I*; World Scientific: Singapore, 1995. p 155.
38. E. Gross, J. Dobson, and M. Petersilka, Density functional theory of time-dependent phenomena, *Top. Curr. Chem.*, 1996, **181**, 81-172.
39. F. A. S. Chipem and G. Krishnamoorthy, Comparative theoretical study of rotamerism and excited state intramolecular proton transfer of 2-(2'-Hydroxyphenyl)benzimidazole, 2-(2'-Hydroxyphenyl)imidazo[4,5-b]pyridine, 2-(2'-

- Hydroxyphenyl)imidazo[4,5-c] pyridine and 8-(2'-Hydroxyphenyl)purine, *J. Phys. Chem. A*, 2009, **113**, 12063-12070.
40. F. A. S. Chipem, N. Dash, and G. Krishnamoorthy, Role of nitrogen substitution in phenyl ring on excited state intramolecular proton transfer and rotamerism of 2-(2-Hydroxyphenyl) benzimidazole: A theoretical study. *J. Chem. Phys.* 2011, **134**, 104308.
41. A. D. Becke, Density-functional thermochemistry. 3. The role of exact Exchange, *J. Chem. Phys.*, 1993, **98**, 5648–5652.
42. C. Lee, W. Yang, and R. G. Parr, Development of the colle-cavetti correlation-energy formula into a functional of the electron-eensity, *Phys. Rev. B*, 1988, **37**, 785–789.
43. T. Yanai, D. P. Tew and N. C. Handy, A new hybrid exchange–correlation functional using the Coulomb-attenuating method (CAM-B3LYP). *Chem. Phys. Lett.* 2004, **393**, 51–57.
44. S. Grimme, J. Antony, S. Ehrlich, and H. Krieg, A consistent and accurate ab initio parametrization of density functional dispersion correction (DFT-D) for the 94 elements H-Pu. *J. Chem. Phys.* 2010, **132**, 154104-154118.
45. J. E. Kwon and S. Y Park, Advanced organic optoelectronic materials: Harnessing excited-state intramolecular proton transfer (ESIPT) process, *Adv. Mater.*, 2011, **23**, 3615-3642.
46. J. Wu, W. Liu, J. Ge, H. Zhang and P. Wang, New sensing mechanisms for design of fluorescent chemosensors emerging in recent years, *Chem. Soc. Rev.*, 2011, **40**, 3483-3495.
47. A. El Nahhas, T. Pascher, L. Leone, L. Panzella, A. Napolitano, and V. Sundstrom, Photochemistry of pheomelanin building blocks and model chromophores: Excited-

- state intra- and intermolecular proton transfer, *J. Phys. Chem. Lett.*, 2014, **5**, 2094-2100.
48. N. Alarcos, J. Angel Organero, F. Sanchez and A. Douhal, Exploring the photobehavior of nanocaged monomers and H- and J-aggregates of a proton-transfer dye within NaX and NaY zeolites. *J. Phys. Chem. C*, 2014, **118**, 8217-8226.
49. Xi.-F. Yang, Q. Huang, Y. Zhong, Z. Li, H. Li, M. Lowry, J. O. Escobedo, and R. M. Strongin, A dual emission fluorescent probe enables simultaneous detection of glutathione and cysteine/homocysteine, *Chem. Sci.*, 2014, **5**, 2177-2183.
50. G. Krishnamoorthy and S. K. Dogra, Twisted intramolecular charge transfer of 2-(4'-N, N-dimethylaminophenyl)pyrido[3,4-d]imidazole in cyclodextrins: Effect of pH, *J. Phys. Chem. A*, 2000, **104**, 2542-2551.
51. G. Krishnamoorthy and S. K. Dogra, Effect of micelles on dual fluorescence of 2-(4'-N,N-dimethylaminophenyl) pyrido[3,4-d]imidazole, *Chem. Phys. Lett.*, 2000, **323**, 234-242.
52. S. Jana, S. Dalapati, and N. Guchhait, N. Proton Transfer assisted charge transfer phenomena in photochromic schiff bases and effect of -NEt₂ groups to the anil schiff bases, *J. Phys. Chem. A*, 2012, **116**, 10948-10958.
53. Y. Kim, M. Yoon, and D. Kim, Excited-state intramolecular proton transfer coupled-charge transfer of p-N, N-Dimethylaminosalicylic acid in aqueous Beta-cyclodextrin solutions. *J. Photochem. Photobiol. A*, 2001, **138**, 167-175.
54. A. Mishra, S. Sahu, N. Dash, S. K. Behera, and G. Krishnamoorthy, Double proton transfer induced twisted intramolecular charge transfer emission in 2 - (4' - N,N-dimethylaminophenyl)imidazo[4,5-b]pyridine. *J. Phys. Chem. B*, 2013, **117**, 9469-9477.

55. V. Vetokhina, J. Nowacki, M. Pietrzak, M. F. Rode, A. L. Sobolewski, J. Waluk, and J. Herbich, 7-Hydroxyquinoline-8-carbaldehydes. 2. Prototropic Equilibria. *J. Phys. Chem. A*, 2013, **117**, 9147-9155.
56. G. Krishnamoorthy and S.K. Dogra, Spectral characteristics of the various prototropic species of 2-(4'-N, N-Dimethylaminophenyl)pyrido[3,4-d]imidazole. *J. Org. Chem.*, 1999, **64**, 6566-6574.
57. R. Pomès, *Proton Relay in Membrane Proteins in 'Molecular Bioenergetics, Simulations of Electron, Proton, and Energy Transfer'*; American Chemical Society: 2004. pp 159-173.
58. M. Itoh, T. Adachi, and K. Tokumura, Transient absorption and 2-step Laser excitation fluorescence- spectra of the excited - state and ground - state proton - transfer in 7-hydroxyquinoline, *J. Am. Chem. Soc.*, 1983, **105**, 4828-4829.
59. R. Schipfer, O. S. Wolfbeis, and A. Knierzinger, P^H - Dependent fluorescence spectroscopy. 12. flavone, 7-hydroxyflavone, and 7-methoxyflavone, *J. Chem. Soc. Perkin Trans.*, 1981, **2**, 1443-1448.
60. H. A. Benesi and J. H. Hildebrand, A Spectrophotometric investigation of the interaction of iodine with aromatic hydrocarbons, *J. Am. Chem. Soc.*, 1949, **71**, 2703-2707.
61. K. Kim and J.-I. Hoe, DFT conformational study of calix [6]arene: Hydrogen bond, *Bull. Korean Chem., Soc.*, 2009, **30**, 837-845.
62. G. Krishnamoorthy, *Hydrogen Bonding and Transfer in the Excited State*; John Wiley & Sons Ltd: 2011. Vol. 1, pp 313-327.
63. Y. Kim and M. Yoon, Intramolecular hydrogen bonding effect on the excited-state intramolecular charge transfer of p-aminosalicylic acid, *Bull. Kor. Chem. Soc.*, 1998, **19**, 980-985.

Figure/Scheme Captions

Figure. 1 Normalised emission spectra of DMAPIP-PyMe in some selected solvents: (1) cyclohexane (2) tetrahydrofuran (3) DMF (4) Acetonitrile, (5) butanol, (6) DMSO, (7) methanol ($\lambda_{\text{exc}} = 355 \text{ nm}$).

Figure. 2 Normalised emission spectra of DMAPIP-ImMe in some selected solvents: (1) cyclohexane (2) tetrahydrofuran (3) acetonitrile, (4) DMSO, (5) propanol, (6) methanol, (7) DMF ($\lambda_{\text{exc}} = 320 \text{ nm}$).

Figure. 3 Absorption spectra of DMAPIP-c in neutral ($0 \mu\text{M F}^-$) and anion ($175 \mu\text{M F}^-$) forms in acetonitrile.

Figure. 4 Fluorescence spectra of DMAPIP-c at different fluoride ion concentration in acetonitrile ($\lambda_{\text{exc}} = 330 \text{ nm}$).

Figure. 5 Absorption spectra of DMAPIP-c in acetonitrile-methanol mixture.

Figure. 6 Normalized Fluorescence spectra of DMAPIP-c in acetonitrile-methanol mixture ($\lambda_{\text{exc}} = 340 \text{ nm}$).

Figure. 7 Benesi-Hilderbrand plot showing 1:3 binding of DMAPIP-c and methanol (measured at TICT band).

Figure. 8 Normalized Fluorescence spectra of PIP-c in acetonitrile-methanol mixture ($\lambda_{\text{exc}} = 290 \text{ nm}$).

Figure. 9 Excited state optimized structures of different forms of DMAPIP-c. $(\text{CH}_3\text{OH})_3$ complex.

Figure. 10 The frontier molecular orbitals of normal planar and dimethylamino twisted tautomer of DMAPIP-c involved in the formation of S_1 state.

Scheme 1 The path for the formation of TICT state via anion.

Scheme 2 Energy level diagram of different forms of DMAPIP-c. $(\text{CH}_3\text{OH})_3$ complex shown in Figure 9.

Table 1 Calculated energy (eV) obtained for the normal emission

Methods	Functional	Normal Emission
CIS/TDDFT	B3LYP	3.45
CIS/TDDFT	CAM-B3LYP	3.70
CIS/TDDFT	B3LYP- D3	3.43
TDDFT	B3LYP	3.21
TDDFT	CAM-B3LYP	3.41
TDDFT	B3LYP-D3	3.20

Experimental value for Normal emission 3.13 eV

Table 2 Absorption band maxima ($\lambda_{\max}^{\text{ab}}$, nm), $\log \epsilon_{\max}$ (in the parenthesis), fluorescence band maxima ($\lambda_{\max}^{\text{fl}}$, nm) and fluorescence lifetimes (τ_{f} , ns) of DMAPIP-c, DMAPIP-ImMe and DMAPIP-PyMe.

Solvent	DMAPIP-c ^a			DMAPIP-ImMe			DMAPIP-PyMe		
	$\lambda_{\max}^{\text{ab}}$ (log ϵ_{\max})	$\lambda_{\max}^{\text{fl}}$	τ_{f}	$\lambda_{\max}^{\text{ab}}$ (log ϵ_{\max})	$\lambda_{\max}^{\text{fl}}$	τ_{f}	$\lambda_{\max}^{\text{ab}}$	$\lambda_{\max}^{\text{fl}}$	τ_{f}
Cyclohexane	327, 341	350, 367, 384	-	278, 300	318, 344	2.2	321, 339, 360	397, 425, 456	2.2
Tetrahydrofuran	332 (4.45)	380	0.80	322 (4.25)	411	1.8	351	440	2.4
Acetonitrile	335 (4.45)	391	0.96	314 (4.28)	424	1.7	349	480	2.5
DMF	336 (4.40)	392	1.41	321 (3.84)	437	1.9	348	470	3.0
DMSO	340 (4.38)	402	1.45	322 (3.73)	432	1.9	356	486	3.2
1-Butanol	339 (4.49)	391	0.74	320 (3.70)	431	1.7	360	484	3.1
1-Propanol	339 (4.49)	393	1.0, 2.4	320 (3.95)	431	1.6	361	482	3.4
Methanol	341 (4.47)	398, 475	0.35, 1.85	316 (4.16)	437	1.8	358	490	3.2

^a Spectral data in dimethylformamide (DMF) and dimethylsulphoxide (DMSO) are from present study and in other solvents are from Ref. 25

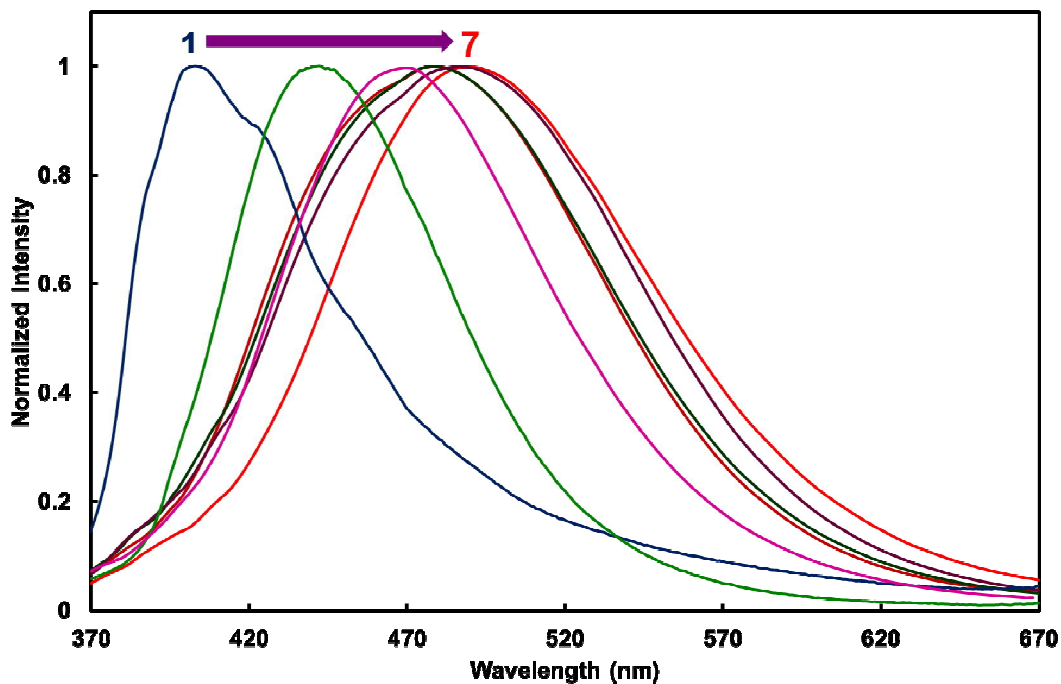


Fig. 1. Normalised emission spectra of DMAPIP-PyMe in some selected solvents: (1) cyclohexane (2) tetrahydrofuran (3) DMF (4) Acetonitrile, (5) butanol, (6) DMSO, (7) methanol ($\lambda_{\text{exc}} = 355$ nm).

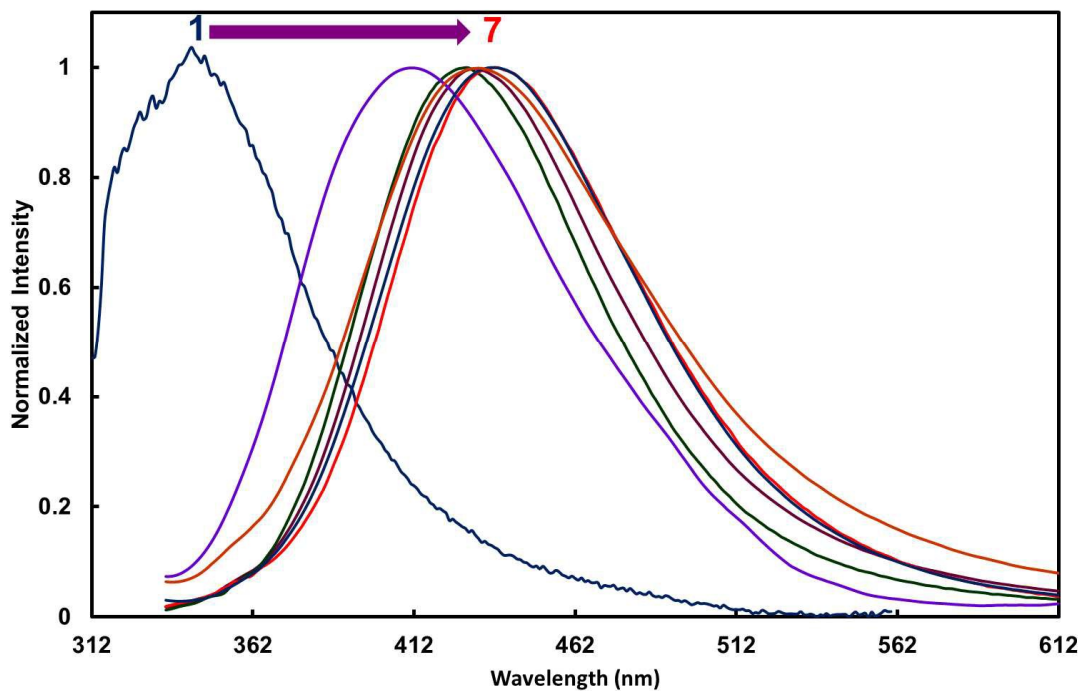


Fig. 2. Normalised emission spectra of DMAPIP-ImMe in some selected solvents: (1) cyclohexane (2) tetrahydrofuran (3) acetonitrile, (4) DMSO, (5) propanol, (6) methanol, (7) DMF ($\lambda_{\text{exc}} = 320$ nm).

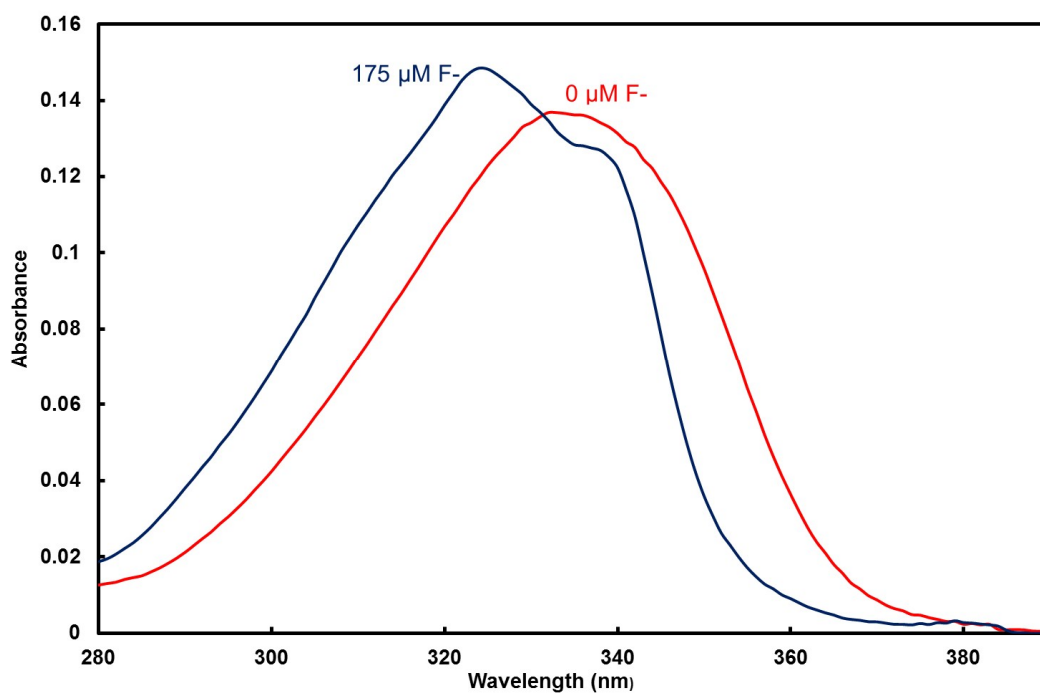


Fig. 3. Absorption spectra of DMAPIP-c in neutral ($0\mu\text{M F}^-$) and anion ($175\mu\text{M F}^-$) forms in acetonitrile.

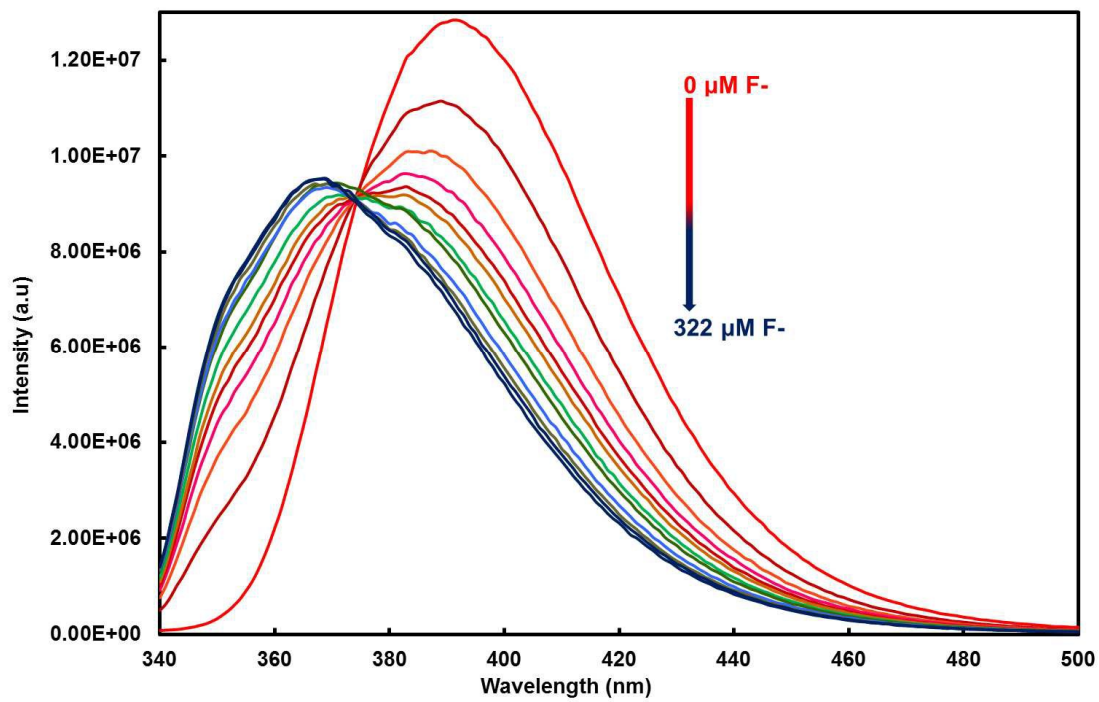


Fig. 4. Fluorescence spectra of DMAPIP-c at different fluoride ion concentration in acetonitrile ($\lambda_{\text{exc}} = 330 \text{ nm}$).

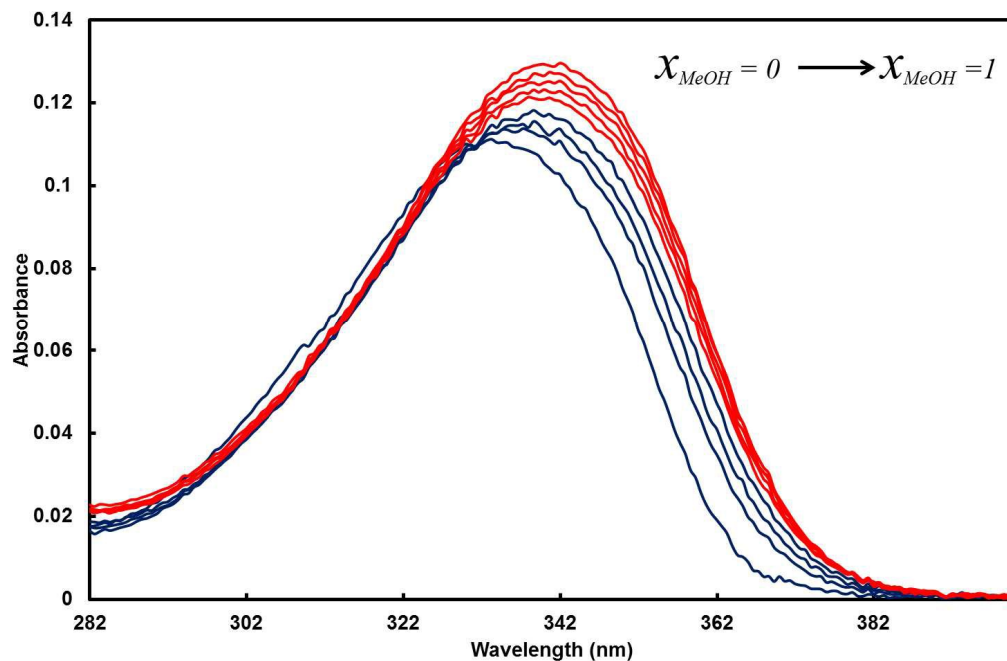


Fig. 5. Absorption spectra of DMAPIP-c in acetonitrile-methanol mixture.

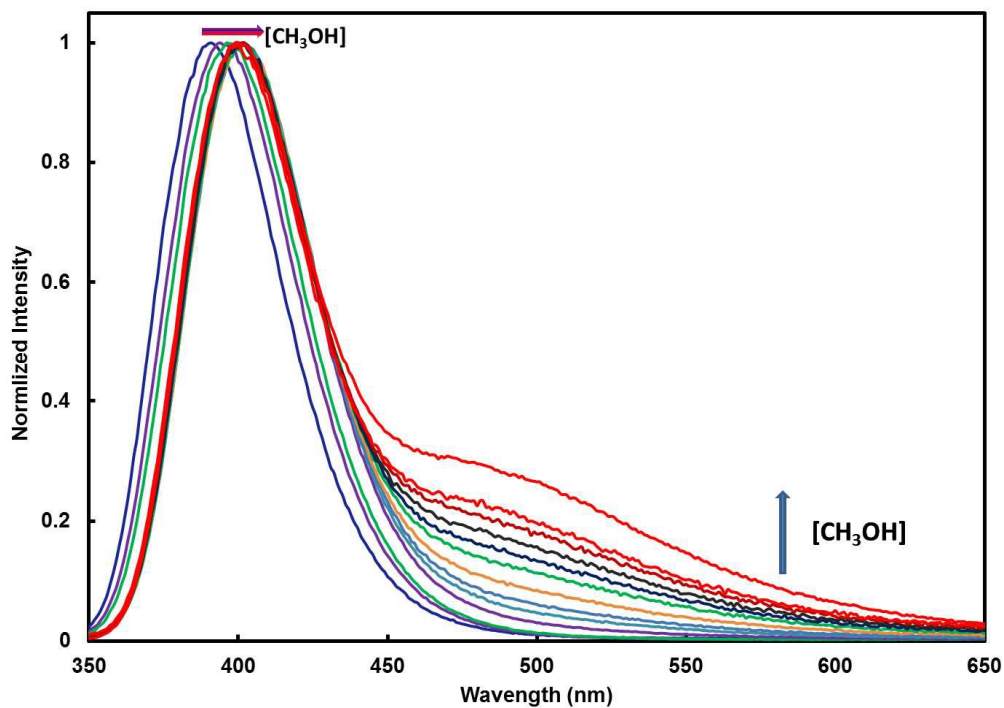


Fig. 6. Normalized Fluorescence spectra of DMAPIP-c in acetonitrile-methanol mixture ($\lambda_{exc} = 340$ nm).

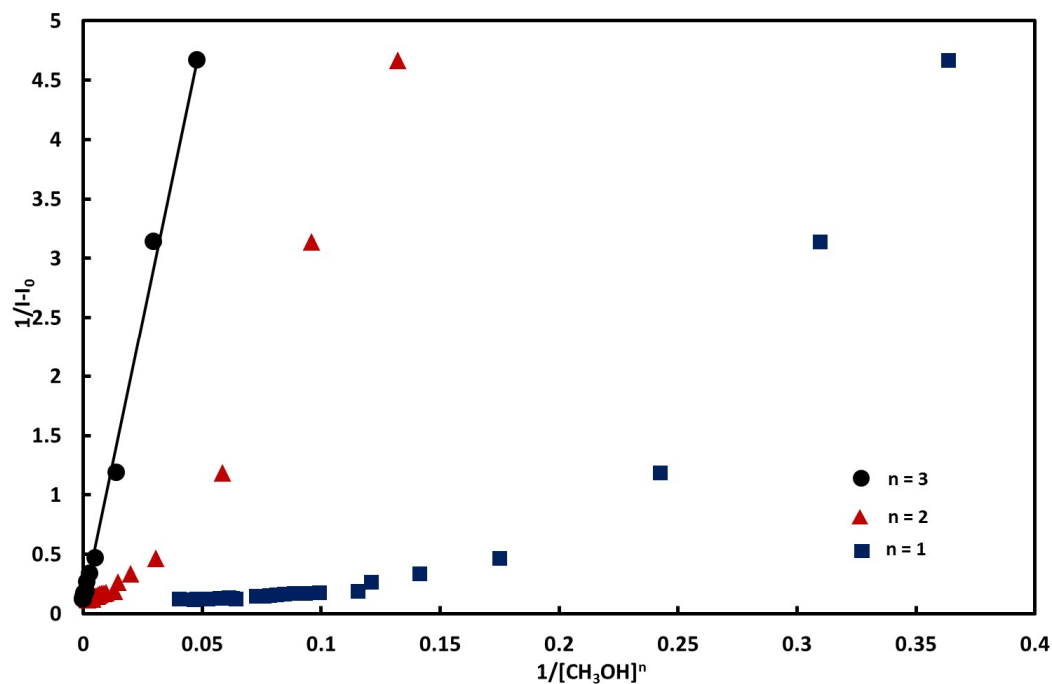


Fig. 7. Benesi-Hilderbrand plot showing 1:3 binding of DMAPIP-c and methanol (measured at TICT band).

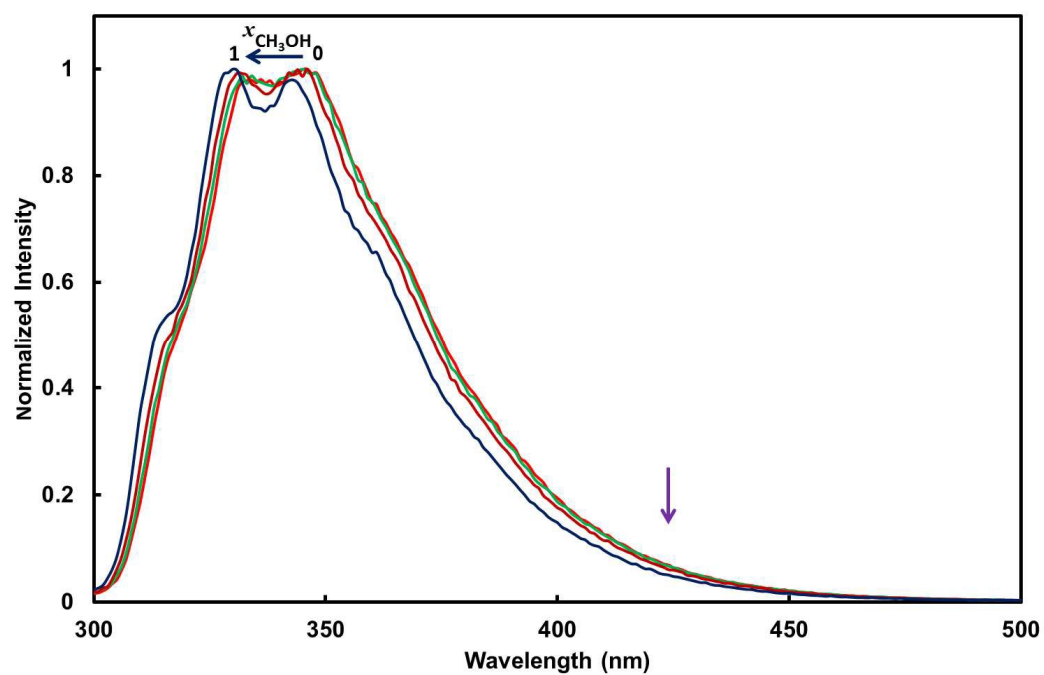


Fig. 8. Normalized Fluorescence spectra of PIP-c in acetonitrile-methanol mixture ($\lambda_{\text{exc}} = 290$ nm).

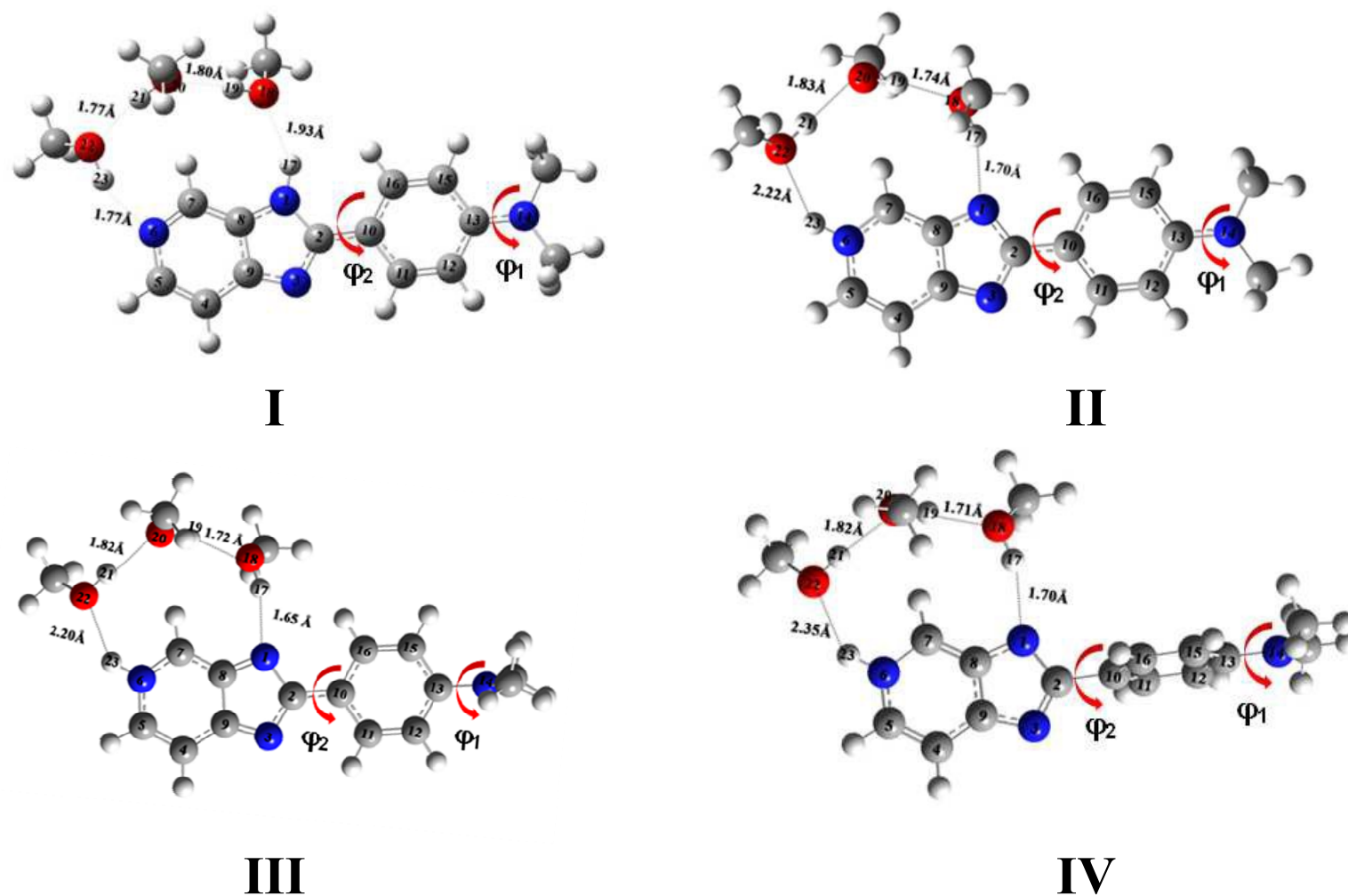


Fig. 9. Excited state optimized structures of different forms of DMAPIP-c. $(\text{CH}_3\text{OH})_3$ complex.

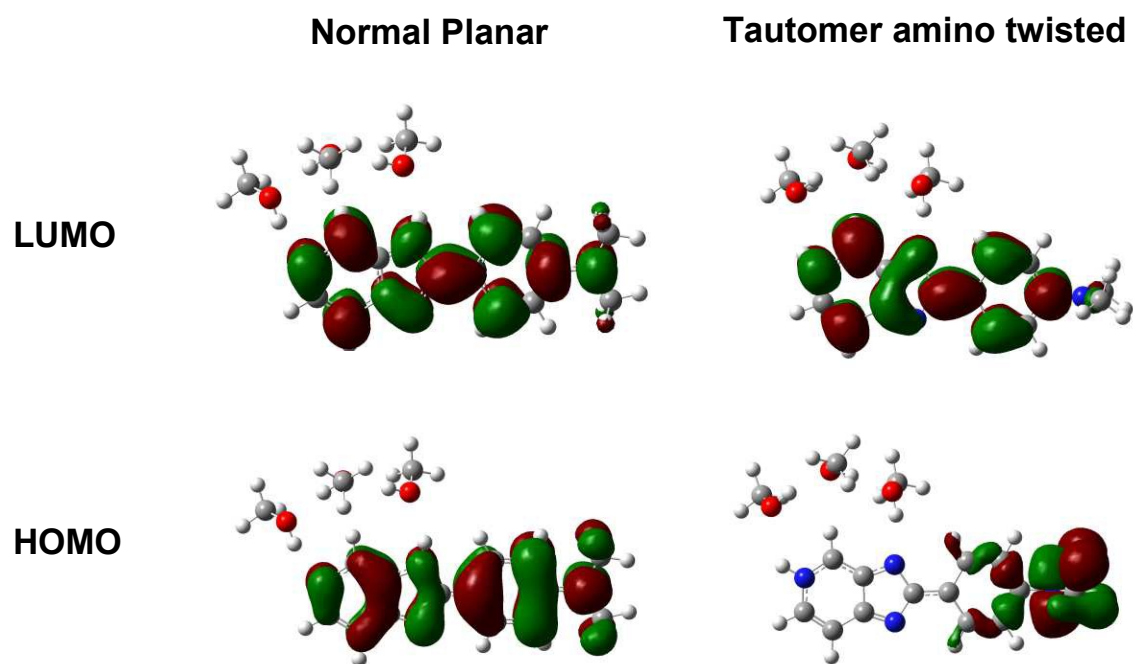
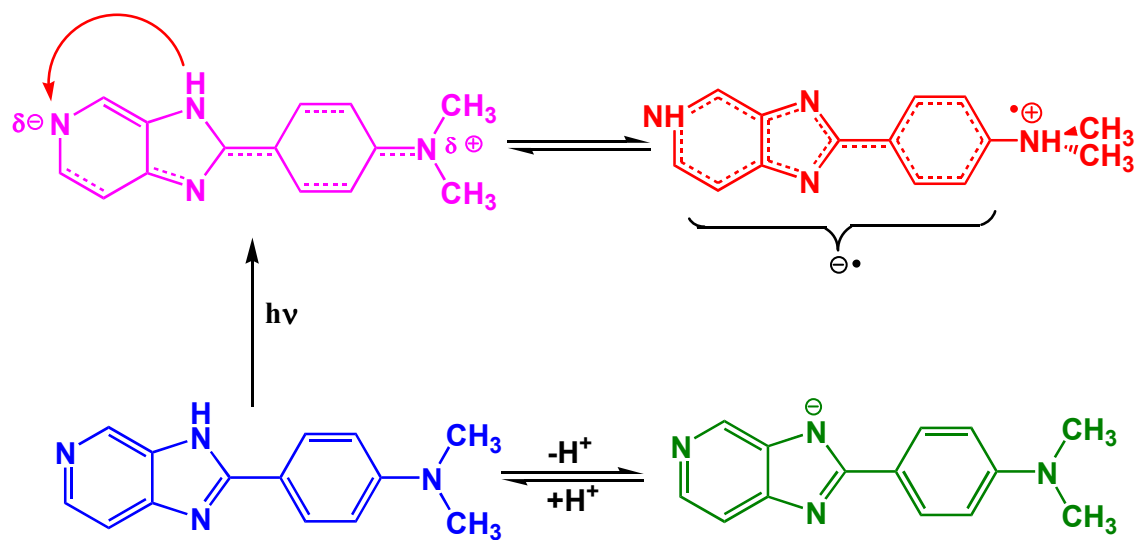
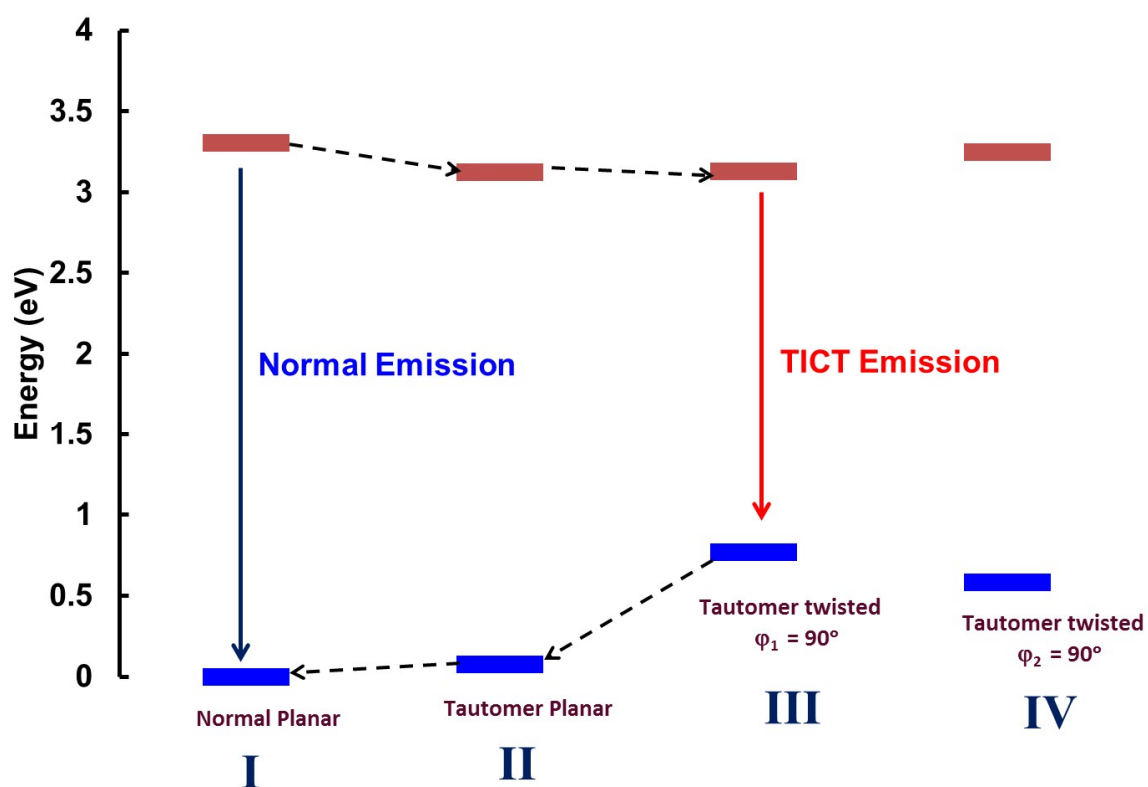


Fig. 10. The frontier molecular orbitals of normal planar and dimethylamino twisted tautomer of DMAPIP-c involved in the formation of S_1 state.



Scheme 1. The path for the formation of TICT state via anion.



Scheme 2. Energy level diagram of different forms of DMAPIP-c.(CH₃OH)₃ complex shown in Fig.7

